ELSEVIER

Journal of Hazardous Materials 142 (2007) 786–796

Journal of Hazardous Materials

www.elsevier.com/locate/jhazmat

Flashing liquid jets and two-phase droplet dispersion I. Experiments for derivation of droplet atomisation correlations

Vincent Cleary [a,*], Phil Bowen [a], Henk Witlox [b]

[a] *Cardiff University, Cardiff, UK*
[b] *DNV Software, UK*

Available online 5 July 2006

Abstract

The large-scale release of a liquid contained at upstream conditions above its local atmospheric boiling point is a scenario often given consideration in process industry risk analysis. Current-hazard quantification software often employs simplistic equilibrium two-phase approaches.

Scaled water experiments have been carried out measuring droplet velocity and droplet size distributions for a range of exit orifice aspect ratios (*L*/*d*) and conditions representing low to high superheat. 2D Phase-Doppler Anemometry has been utilised to characterise droplet kinematics and spray quality. Droplet size correlations have been developed for non-flashing, the transition between non-flashing and flashing, and fully flashing jets. Using high-speed shadowography, transition between regimes is defined in terms of criteria identified in the external flow structure. An overview companion paper provides a wider overview of the problem and reports implementation of these correlations into consequence models and subsequent validation.

The fluid utilised throughout is water, hence droplet correlations are developed in non-dimensional form to allow extrapolation to other fluids through similarity scaling, although verification of model performance for other fluids is required in future studies. Data is reduced via non-dimensionalisation in terms of the Weber number and Jakob number, essentially representing the fluid mechanics and thermodynamics of the system, respectively.

A droplet-size distribution correlation has also been developed, conveniently presented as a volume undersize distribution based on the Rosin–Rammler distribution. Separate correlations are provided for sub-cooled mechanical break-up and fully flashing jets. This form of correlation facilitates rapid estimates of likely mass rainout quantities, as well as full distribution information for more rigorous two-phase thermodynamic modelling in the future.

Keywords: Sub-cooled; Superheated; Flashing; Atomisation; Correlation; Droplet-size distribution

1. Introduction

When a liquid contained at conditions above the ambient saturation pressure is released to the atmosphere the liquid is described as ‘superheated’. Rapid boiling of the resultant liquid jet occurs, producing two-phase flow. Under suitable conditions, dynamic expansion of vapour bubbles shatters the liquid stream to produce a finely atomised spray. This phenomenon, known as ‘flashing’, gives rise to potentially explosive and certainly hazardous heterogeneous two-phase clouds.

When a liquid is released to the atmosphere below the ambient saturation pressure the liquid is described as ‘sub-cooled’. Break-up of the resultant jet is dominated by aerodynamic and surface tension forces at the liquid/air interface. This phenomenon, known as ‘mechanical break-up’, occurs when any random protrusion on the surface of a jet is subjected to a lower gas pressure over its crest than at its base [1]. The faster the jet relative to the surrounding atmosphere the more pronounced the effect. Eventually this protrusion may detach from the jet to form a droplet.

Whether a release occurs under sub-cooled or superheated conditions, rainout of larger droplets creates a spreading vapourising pool in the vicinity of the release orifice and determines the amount of material that remains airborne as the cloud disperses. A certain percentage of rained-out material will evaporate from the spreading pool and reattach itself to the dispersing cloud, potentially more dangerously as vapour. The liquid that remains on the ground presents its own hazard, as for example it

* Corresponding author. Tel.: +44 2920 875792.
E-mail address: ClearyV@Cardiff.ac.uk (V. Cleary).

0304-3894/$ – see front matter © 2006 Elsevier B.V. All rights reserved.
doi:10.1016/j.jhazmat.2006.06.125

Nomenclature

C_d	discharge coefficient
C_{pL}	specific heat of liquid (J kg^{-1} K^{-1})
d_p	droplet particle diameter (m)
d_0	nozzle orifice diameter (m)
h_{fh}	latent heat of vapourisation (J kg^{-1})
Ja	Jakob number = $(\rho_L C_{pL} \Delta T_{sh})/(\rho_v h_{fg})$
L	axial length of nozzle (m)
Re	Reynolds number = $\rho u_0 d_0/\mu$
SMD	(Global) Sauter mean diameter = $\sum d_p^3 / \sum d_p^2$ (m)
ΔT_{sh}	superheat (°C)
u_o	mean axial velocity along the orifice [=mass flow rate/(orifice area × liquid density] (m s^{-1})
$v(D)$	fraction of total volume of spray contained in droplets of size less then D
We	Weber number $\rho u_0^2 d_0/\sigma$

Greek letters

μ	dynamic viscosity (Pa s)
ρ	density (kg m^{-3})
σ	surface tension (N m^{-2})
ϕ	correction factor for Jacob number

Subscripts

a	atmospheric
L	liquid
o	orifice
v	vapour

can ignite to create a pool fire. For the purposes of accurate hazard quantification it is therefore necessary to be able to predict the behaviour of droplets in accidental releases of these kinds.

There are various empirical correlations for mechanical break-up proposed in literatures [2–7] though most consider conditions outside the domain of interest for hazard analysis. In addition, most dispersion hazard models currently utilise some form of the 'critical Weber number' criterion to estimate maximum sizes for stable droplets from mechanical break-up, see Eq. (1).

$$We_{crit} = \frac{\rho_a u_0^2 d_p}{\sigma_L} = 10\text{–}20 \quad (1)$$

While this methodology is appropriate for single droplet situations it is not considered appropriate for this application.

Several authors [8,9] have reported little or no discernible difference between jet releases under conditions of 'low' superheat and mechanical break-up. Under these conditions the effect of bubble nucleation appears to be negligible so that mechanical break-up prevails, or restricted to the external break-up mode where bubbles are generated and grow within the jet downstream of the exit orifice. Hence, flashing appears to be limited by a transition superheat limit, allowing mechanical break-up mechanisms to dominate into the superheated region.

Kitamura et al. [9] propose a transitional correlation using superheated water and ethanol flowing through 'long' nozzles ($50 < L/d_0 < 115$) and flashing into an evacuated chamber,

$$Ja\,\phi = 100\, We_v^{-1/7}, \quad \text{with} \quad \phi = 1 - e^{-2300(\rho_v/\rho_L)} \quad (2)$$

This correlation is claimed to govern transition to 'complete' flashing, where ϕ is a function of the ratio of vapour to liquid density.

Muralidhar et al. [10] propose a simple model that describes a transition point between mechanical break-up and flashing atomisation based on a critical superheat above which the rate of change of rainout falls sharply in accordance with a rapidly decreasing droplet size in the spray.

However, beyond the initial transition superheat several further stages of transition are likely to exist until a final stage of atomisation is reached. For example, Park and Lee [11] identify three intermediary junctures of flashing. What is unclear is how rapid the evolution from the initial transition stage to the final transition stage occurs, and which stage is represented by the equation proposed by Kitamura et al.

It is necessary, therefore, to formulate a model governing jet break-up across the full spectrum of upstream conditions, including the establishment of valid criteria governing the various stages of transition from mechanical break-up to flashing atomisation.

Given financial and safety constraints, water is used as the model fluid. Hence, at this stage predictions for other liquids rely on the established non-dimensional variables adopted within the model. Further work on other fluids will be required to validate this assumption.

The current paper reports the derivation of droplet atomisation correlations from scaled water experiments. See the companion paper [12] for a wider overview of the problem and implementation of these correlations into consequence models and subsequent validation. Section 2 of this paper describes the experimental procedure and range of experiments. Section 3 describes the results of the data analysis for the experiments and proposes new SMD and droplet-size correlations for sub-cooled jets, fully flashing jets and transition to fully flashing. The overall SMD correlation is summarised in Section 4 and final conclusions are presented in Section 5.

2. Experimental procedure

Sharp-edged brass nozzles were manufactured in-house, with care taken to avoid the formation of aberrations or inaccuracies on the nozzle inlet as recent work [13] has indicated that these influence the internal flow characteristics and significantly alter the atomisation process. The length of the final orifice geometry is defined to be consistent with that defined in standard atomisation and jet break-up literature [8,9].

Droplet size and velocity measurements were made for both the sub-cooled and superheated rig using a DANTEC 1D Phase Doppler Anemometry (PDA) system mounted on a computer controlled mechanical traverse. Measurements are made based on phase Doppler interferometric theory, whereby light from two

incident laser beams is scattered by particles entering the measurement volume, defined by the intersection of the two beams. Receiving optics placed at a specific off-axis location project the scattered light onto multiple photo-detectors. The frequency of each Doppler burst is proportional to the particle velocity and the phase shift between signals from different detectors is directly proportional to the particle diameter.

A range of optical configurations were appraised before the final system was specified. This was necessary due to the broad range of droplet sizes produced by some of the sprays. The optimum optical set-up for sub-cooled releases consisted of 600 mm focal length lenses and a beam separation of 20 mm, which gave a diameter range of 0–1480.2 μm. A bandwidth of 12.0 MHz enabled particle velocities in the range −46.3 to 138.9 m s^{-1} to be measured. For superheated releases 600 mm focal length lenses and a beam separation of 30 mm gave a diameter range of 0–385 μm. Again a 12.0 MHz bandwidth was adopted which in this case enabled particle velocities in the range −30.8 to 92.6 m s^{-1} to be measured.

Due to the poor atomisation quality for low-pressure sub-cooled release conditions, validation rates were relatively low. Typical validation rates for sub-cooled sprays ranged from 20 to 40% at low pressure, i.e. 4 bar, and 60–90% at high pressure, i.e. 24 bar. However validation rates for flashing releases were typically in the range 70–95%. Validation rates varied inversely with spray density throughout the spray cross-section, i.e. validation rates were at their highest at the edge of the spray where the spray density was at its minimum, and vice versa. The poor quality of the spray for sub-cooled conditions also presented challenges in terms of data truncation. These issues were minimised by the adopted optical configuration, however it is never possible to be completely confident that truncation has been eliminated for low-quality sub-cooled jets. By contrast for superheated releases it appeared possible to completely eliminate data truncation, as each measured sample was less than 200 μm, almost half the upper diameter size afforded by the associated optical set-up.

For both sub-cooled and superheated sprays PDA data was taken at regular horizontal increments through the spray in the plane of the central axis. The necessity to represent the distribution as a whole by a single number requires that measurements taken at these radial locations be transformed to a ‘global’ measurement. At each radial location the PDA system recorded 20,000 ‘validated’ samples. However, because of this and the non-uniformity of the droplet concentration through the spray it was not possible to take a mean in order to provide this single number. Instead a comprehensive approach was adopted for the globalisation of the local measurements. Radial values are normalised by the flux in order to counter the variation in droplet concentration through the spray cross-section, and by the absolute validation rate so that proportionately each global measurement is based on the same number of samples. However, this approach necessitates that the samples rejected by the PDA system have the same distribution characteristics as those accepted.

The sub-cooled spray rig essentially consisted of a steel tank, with a working capacity of 200 l, and a vertically positioned nozzle adaptor, which allowed nozzles of various orifice geometries to be used according to the needs of the experiment. The nozzle was positioned vertically so as to negate any gravitational effects on the spray. Water was circulated using a centrifugal vertical pump and the pressure was regulated using a pressure gauge and a pressure relief valve. Table 1 summarises the programme of experimental work carried out for the investigation of sub-cooled jets.

Table 1
Sub-cooled program

Gauge pressure (bar)	Nozzle diameter (mm)	Aspect ratio (L/d_0)
$4 \le P \le 20$ at 2 bar increments	2.00	1.7 3.5
$4 \le P \le 24$ at 2 bar increments	1.00	3.4 7.0 10.0 20.0 30.0 50.0
0.75	4.53 9.33	

Findings from automotive injector studies of simple atomisers usually quote that the jet is fully developed after some 75–100 nozzle diameters downstream, though these will be for considerably higher pressures and for jets in the ‘atomisation’ break-up regime. Releases considered in this study invariably fall into the ‘second-wind’ break-up regime. This means that for an appreciable distance downstream the jet does not break-up at all, but in fact remains intact as a ‘pencil’ jet. Hence, fully developed sprays will not be established until further downstream than distances quoted for automotive sprays, i.e. several hundred nozzle diameters. Therefore a compromise is required between the atmospheric dispersion modelling approach of a fully developed spray existing immediately downstream and the reality of a finite break-up length preceding the fully developed spray. In the course of this study post-expansion data was taken at 500 mm downstream of the exit orifice, beyond which point it was assumed that dynamic jet break-up was complete. This is also found to be consistent with previous data produced by Buchlin et al. [14].

The superheated spray rig consists of a sealed pressure vessel with a working capacity of approximately 33 l. Vents in the base of the tank enable refilling. A helical-shaped electrical incoloy heating element is used to heat the water inside the tank. Pressure is created through the expansion of the water (i.e. conditions within the vessel are initially saturated) and hence the flowrate is a function of the water temperature and the orifice geometry. Nozzles are attached to the rig via a conduit elbow at the base of the tank, so that releases are directed parallel to the ground, thereby making gravitational influences on the droplet distribution unavoidable. Jet temperature and pressure are recorded using a thermocouple and a pressure transducer positioned 15 mm upstream of the orifice inlet and connected to a data acquisition system, which records data at 1000 Hz.

The inability of the laser to penetrate sprays produced by nozzles with diameters in excess of 1 mm and lengths in excess of 3.4 mm limited the experimental programme to nozzles of

Table 2
Full flashing programme

Stagnation temperature (°C)	Downstream distance (mm)	Nozzle diameter (mm)	Aspect ratio (L/d_0)
180	250	0.75	4.53
	500 750	1.00	3.40

Table 3
Transition programme

Stagnation temperature (°C)	Nozzle diameter (mm)	Aspect ratio (L/d_0)
130		
140	4	0.85
150	3	1.13
160	2	1.70
170		
180	1	3.40

characteristic geometries shown in Table 2. Using these nozzles it is not possible to produce fully flashing sprays at stagnation temperatures below 180 °C, which is the maximum operating temperature of the superheated rig. For this reason it was only possible to conduct PDA particle sizing for one set of upstream conditions.

The temperature at the exit orifice is transient during the initial stages after the release valve is opened, until equilibrium is reached and the jet exit temperature stabilises below the vessel stagnation temperature. Potential causes of this temperature difference are heat transfer and phase change prior to the orifice exit, the latter being part of an ongoing study. As jet temperature increases, jet break-up passes through the various transition regimes. Combining high-speed (1000 fps) shadowography with the data acquisition system it was possible to couple the observed break-up characteristics with the jet temperature and release pressure.

Backlit shadowgraphs of superheated jets were taken using a NAC 1000 high speed video camera and a VCR, which recorded images at 1000 fps. The jet was backlit using a 1000 W spotlight focused on the jet centreline. An efficient extract system was used to prevent droplet recirculation. Table 3 summarises the series of initial conditions for which images were recorded.

3. Data analysis

3.1. Sub-cooled releases

A correlation for predicting droplet SMD for sub-cooled releases has been produced based on three non-dimensional groups; Weber number, Reynolds number and the nozzle aspect ratio (L/d_0) and takes the form shown in Eq. (3).

$$\frac{\mathrm{SMD}}{d_0} = 64.73\left(\frac{L}{d_0}\right)^{0.114} Re\mathrm{L} - 0.014\, We_{\mathrm{L}}^{-0.533} \quad (3)$$

The effect of the various input parameters on the droplet SMD is demonstrated by Eqs. (4)–(6)

$$\mathrm{SMD} \propto d_0^{0.34} \quad (4)$$

$$\mathrm{SMD} \propto \left(\frac{L}{d_0}\right)^{0.114} \quad (5)$$

$$\mathrm{SMD} \propto P^{-0.54} \quad (6)$$

Droplet SMD was found to depend strongly on the nozzle characteristics; for nozzle aspect ratio an explicit power law relationship has been proposed. However, the effect of nozzle aspect ratio is still a matter of some debate and ongoing research. Far from the trend being uniform, the relationship between droplet SMD and aspect ratio displays a complicated fluctuating trend line. This also reflects recent findings from work undertaken at Cardiff University [15] where a 'wavy' relationship was found to exist between aspect ratio and discharge coefficient, which is itself related to the flow structure of the liquid in the nozzle. In the spirit of 'simplicity' for inclusion in more general atmospheric modelling, a linear relationship has been superimposed across the range of aspect ratios used so that a coherent correlation could be deduced from the data. Fig. 1 demonstrates this visually.

For scenarios where the aspect ratio in a practical release is outside the range considered here it is recommended that a lower cut-off limit of 1.7 and an upper cut-off limit of 50 be adopted. It is reasonable to assume that there must be a lower cut-off because a sharp-edged orifice ($L/d_0 = 0$) produces a spray with a finite SMD. Given the relatively weak dependence of aspect ratio indicated in the correlation for an aspect ratio an order of magnitude less than the lower cut-off limit the maximum error

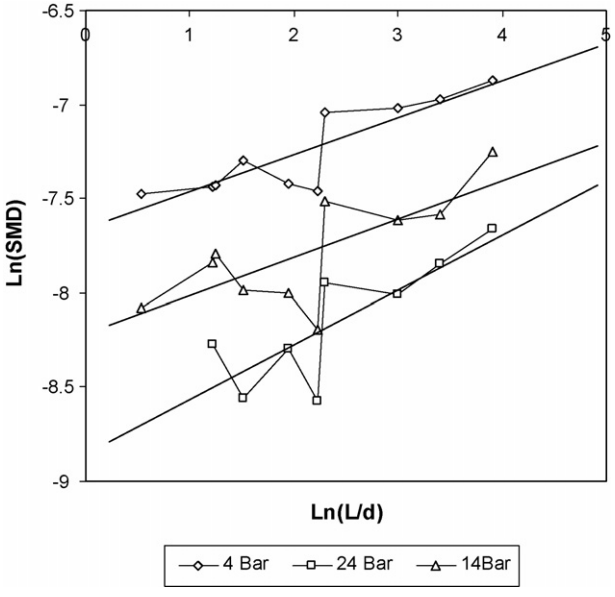

Fig. 1. 'Wavy' relationship between aspect ratio and droplet SMD.

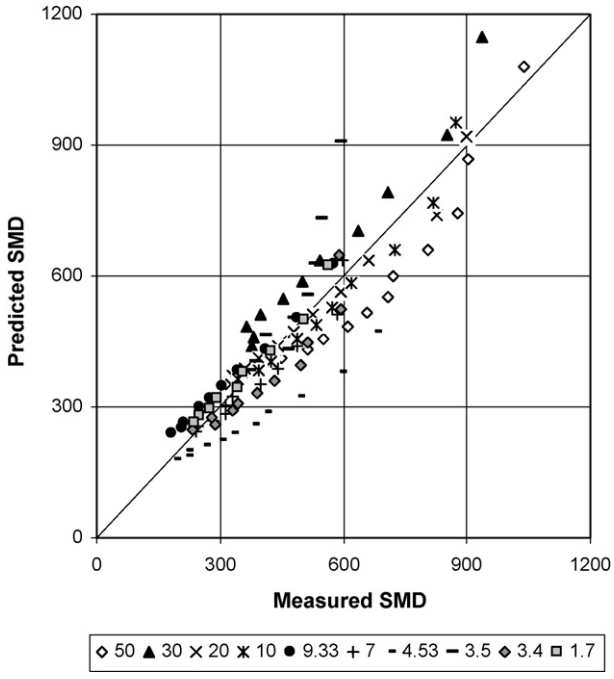

Fig. 2. Comparison of measured and predicted droplet SMD.

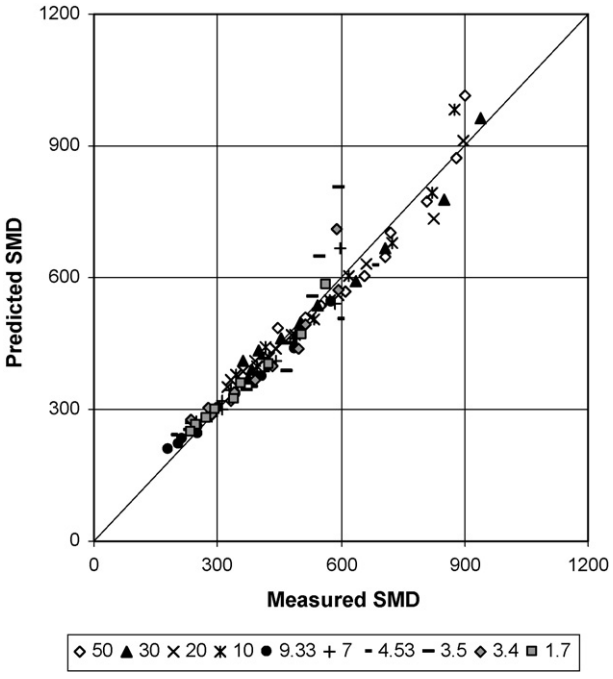

Fig. 3. Improved accuracy using nozzle specific correlations.

in SMD prediction is 30%. Similarly there is physical justification for adopting an upper cut-off limit as one would expect the influence of aspect ratio on downstream spray conditions to eventually diminish. For an aspect ratio an order of magnitude higher than the upper limit the maximum error in SMD is also 30%.

In order to evaluate the accuracy of the proposed correlation, measured data has been plotted against predicted data; this is shown in Fig. 2.

In an attempt to further improve the accuracy of the correlation, nozzle specific correlations can be developed which avoid the ambiguity introduced to the correlation by the unstable relationship demonstrated between the aspect ratio and the droplet SMD. However, this improved accuracy of course comes at the expense of generality. Fig. 3 demonstrates the level of accuracy it is possible to achieve.

A correlation for droplet-size distribution has also been produced based on the common Rosin–Rammler size distribution and is presented in Eq. (7). The correlation is conveniently presented in terms of the droplet SMD and can therefore be readily integrated with the proposed droplet size correlation.

$$1 - v(D) = \mathrm{e}^{-0.3(D/\mathrm{SMD})^{1.6}} \tag{7}$$

Fig. 4 shows the volume undersize distribution for the experimental data, the Rosin–Rammler correlation as presented by Elkotb [7] and the newly proposed Rosin–Rammler correlation for a 24 bar release pressure. Presenting the correlation as a volume undersize function is very useful in terms of atmospheric dispersion modelling, particularly in light of near-field rainout. If one selects a critical droplet size above which all liquid released rains-out, the percentage of the total volume of spray which rains out can be immediately determined from the graph. In general the experimental data and proposed distribution function show negligible volume contained in droplets with diameters of 100 μm or less for the range of initial conditions considered within the scope of this paper. As droplets above 100 μm will rainout, for 'low' to 'medium' release pressures the model predicts that most of the released material will rainout and contribute to pool formation rather than form a potentially hazardous cloud.

3.2. Fully flashing jets

Fully flashing jets have been investigated for the initial conditions outlined in Table 2. In each case the exit temperature of the jet at the nozzle was 155 °C (55 °C superheat). Results

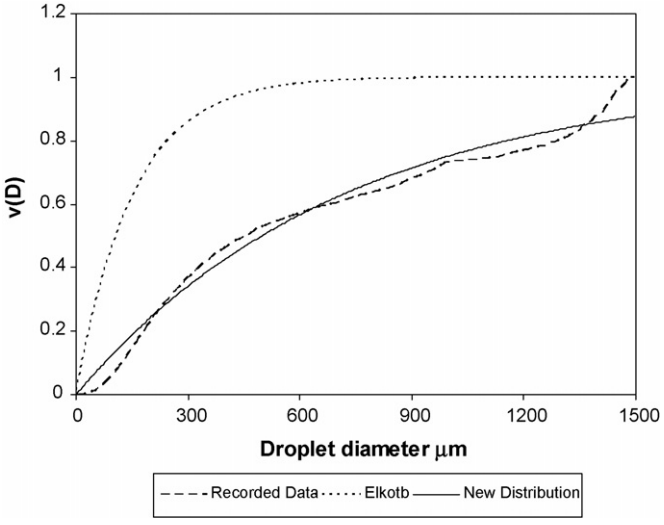

Fig. 4. Sub-cooled volume undersize distribution (24 bar, SMD = 344 μm).

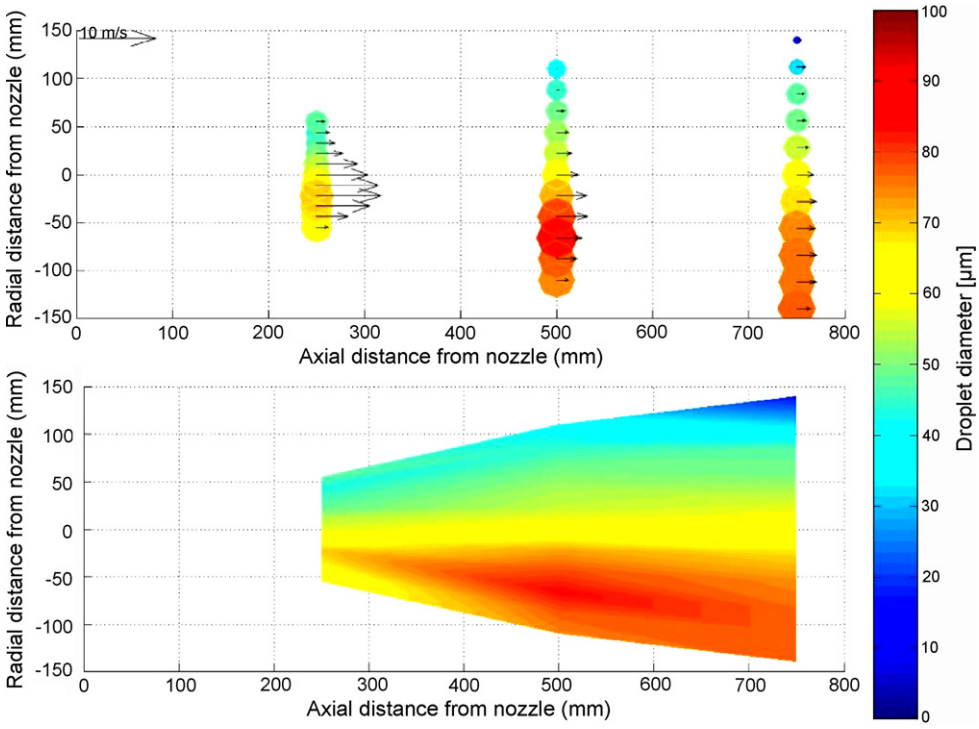

Fig. 5. Distribution of droplet SMDs for 0.75 mm nozzle diameter.

taken using the PDA system have been processed to produce 'cherry plots', which describe the distribution of droplet sizes in the spray; these are presented in Figs. 5 and 6.

Figs. 5 and 6 are presented in two constituent parts so that the first part displays the measured droplet diameters in terms of a colour code according to the scale given on the right hand side of each figure and also scaled so that the size of each circle is proportional to the measured droplet SMD at that spatial location. Velocity vectors are attributed to each circle to indicate the mean axial velocity of the particles at each spatial location. The scale for these vectors is presented in the top left hand corner of each figure. The second part of each figure utilises a function

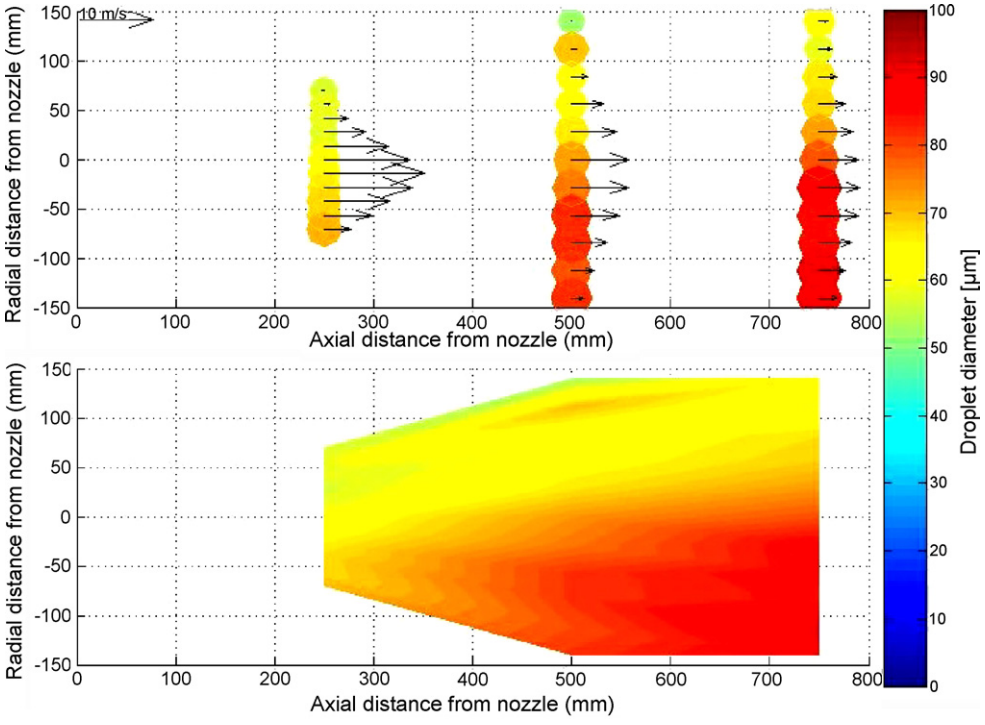

Fig. 6. Distribution of droplet SMDs for 1.00 mm nozzle diameter.

Table 4
Measured global droplet SMD

Nozzle diameter (mm)	Aspect ratio (L/d_0)	Downstream distance (mm)	Global SMD (μm)
0.75	4.53	250	59.5
0.75	4.53	500	71.0
0.75	4.53	750	68.9
1.00	3.40	250	62.8
1.00	3.40	500	71.0
1.00	3.40	750	79.0

of the Matlab programme on which they were produced which interpolates the data between each measurement point to give an estimated droplet size distribution throughout the whole spray.

Physical restrictions imposed on the experimental apparatus caused by the width of the spray produced by the 1.00 mm nozzle diameter prevented measurements being taken in the outer region of the spray beyond 500 mm downstream. For this reason data from the edge of the spray at the furthermost downstream distances is missing. It is likely that the upper portion of the spray would have contained droplets with SMD below 50 μm, which are absent from this dataset.

Figs. 5 and 6 indicate that as droplets progressed further downstream gravitational forces began to influence their trajectory so that larger droplets began to rainout. This is manifested by the cluster of droplet diameters above 80 μm in the lower portion of the spray. This contributes to the apparent trend of droplet growth with downstream distance, as the larger droplets separate from the higher quality spray, leading to the apparent increase in droplet SMD in the downstream direction. This downward migration may also increase the potential for coalescence, which would also have the influence of increasing droplet SMD. In the case of the 0.75 mm nozzle diameter most of these droplets had already rained out at 750 mm downstream. In the case of the 1.00 mm nozzle diameter the increase in orifice size resulted in larger droplets with higher velocities. Consequently droplets in this spray possess increased momentum, which reduced their angle of trajectory and carried them further downstream. For this reason droplets with SMDs above 80 μm (largest circle in plot) were still present in the spray at 750 mm downstream. However, it is still likely that these droplets would have eventually rained out further downstream.

This effect is also demonstrated by the measured global droplet SMDs presented in Table 4, where droplet SMDs are clearly shown to increase with downstream distance (in the case of the 0.75 mm nozzle diameter SMD peaks at 500 mm downstream as larger droplets have rained out at 750 mm downstream). Therefore, for the purposes of atmospheric dispersion modelling, post-expansion data was taken at 250 mm downstream of the exit orifice, at which point it was assumed that dynamic jet break-up was complete and the effect of coalescence and droplet rainout was least significant.

The velocity distributions presented in Figs. 5 and 6 display similar characteristics in each case. At 250 mm downstream the peak of each velocity profile is shifted towards the lower region of the spray, which also contains the larger droplets. This is due

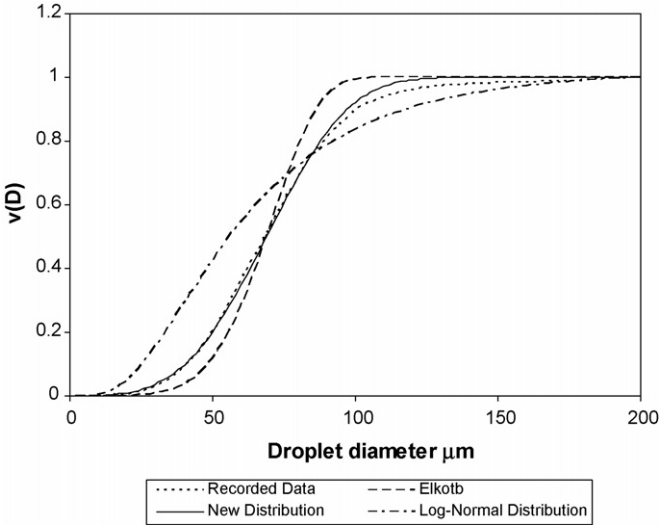

Fig. 7. Fully flashing volume undersize distribution (nozzle = 1 mm, SMD = 62.8 μm).

to the relative impact of aerodynamic drag on droplet trajectory with respect to droplet diameter. It can be seen that at each downstream location that the average droplet velocity is approximately proportional to droplet SMD. As the droplets progress further downstream the velocity reduces and the velocity profiles flatten. The spray produced from the 1 mm nozzle demonstrate higher average droplet velocities than the 0.75 mm case due to the increase in mass flowrate caused by the larger exit orifice.

A correlation for droplet-size distribution for fully flashing sprays has also been produced, based on the common Rosin–Rammler size distribution and is presented in Eq. (8).

$$1 - v(D) = \mathrm{e}^{-0.5(D/\mathrm{SMD})^{3.5}} \tag{8}$$

Fig. 7 shows the volume undersize distribution for the experimental data produced using the 1 mm nozzle at 250 mm downstream. Also included is the log-normal distribution as recommended in literature [16] and presented by Eq. (9).

$$f(d_\mathrm{p}) = \frac{p(t = d_\mathrm{p}/d_\mathrm{pm})}{d_\mathrm{p}}, \quad \text{with}$$

$$p(t) = \frac{1}{(2\pi)^{0.5}\ln(\sigma_\mathrm{G})}\exp\left[-0.5\left(\frac{\ln t}{\ln(\sigma_\mathrm{G})}\right)\right]^2 \tag{9}$$

A more typical distribution profile is observed for fully flashing sprays, which is indicative of a more complete atomisation process compared to sub-cooled jets. The form of the proposed distribution correlation is clearly more suited to the measured droplet distributions. It is also presents an improvement upon the Rosin–Rammler correlation presented by Elkotb [7].

3.3. Transition to flashing

The transition from mechanical break-up to full flashing is demonstrated in Fig. 8. In the images presented, the release pressure is approximately 1.5 bar and the nozzle diameter is 4 mm (aspect ratio 0.85). At 0 °C superheat mechanical break-up is the

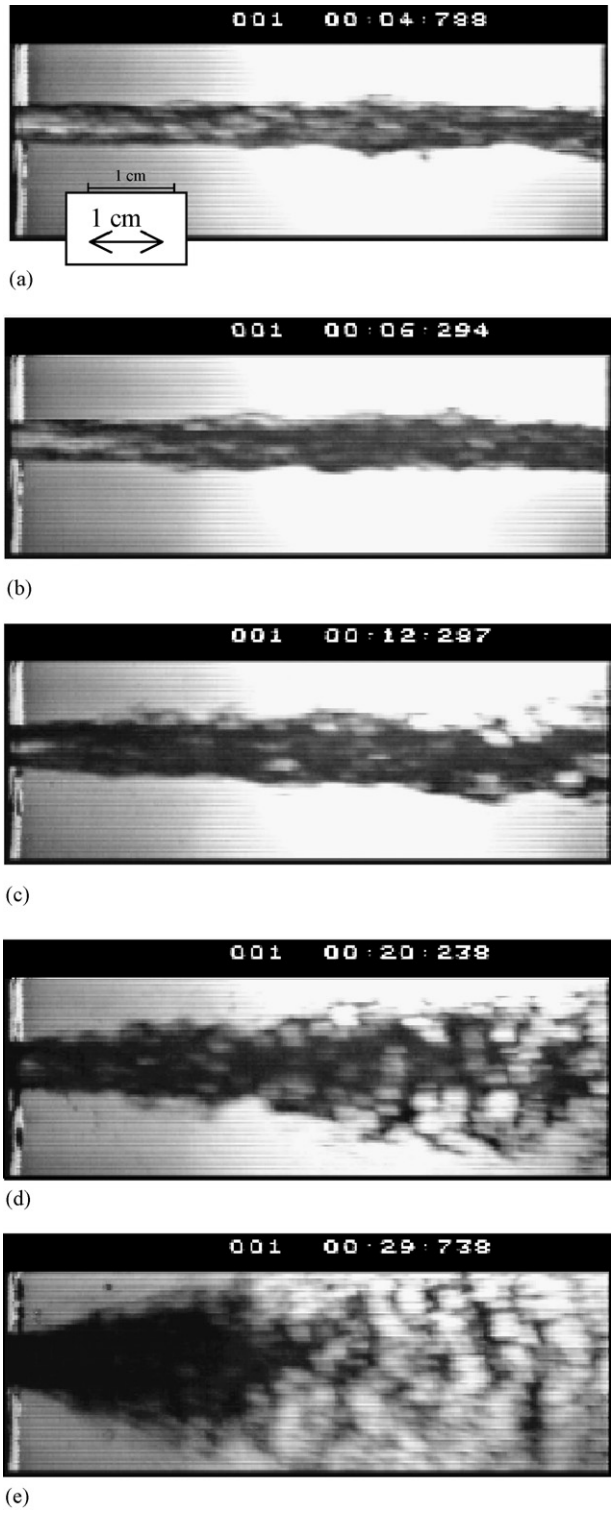

Fig. 8. Evolution of jet break-up with increasing temperature (nozzle = 4 mm, pressure = 1.5 bar). (a) $\Delta T_{sh} = 0\,^{\circ}C$; (b) $\Delta T_{sh} = 5\,^{\circ}C$; (c) $\Delta T_{sh} = 10\,^{\circ}C$; (d) $\Delta T_{sh} = 15\,^{\circ}C$; (e) $\Delta T_{sh} = 17.5\,^{\circ}C$.

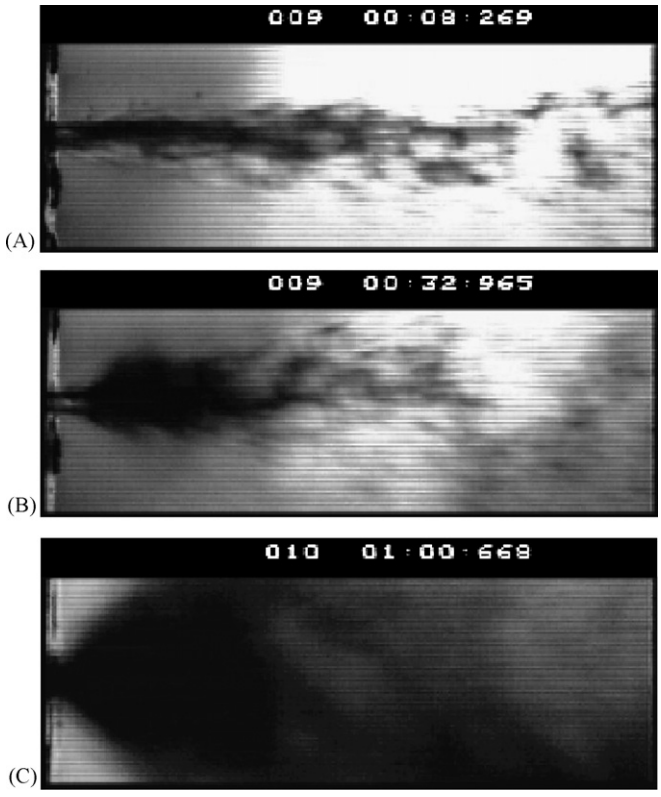

Fig. 9. Stages of transition for superheated jet break-up.

dominant mechanism. At 5 °C bubbles begin to form, causing the jet to swell. At 10 °C bubbles begin bursting at the surface of the jet. Large bubbles are clearly observed within the spray. At 15 °C bubbles bursting in the jet initiate disintegration of the core, with ligament formation at the edges of the spray. At 17.5 °C a wide angled jet has developed beyond the break-up length with rapid bubble growth causing the complete disintegration of the core.

Three distinct stages of transition have been identified and are presented in Fig. 9. Condition A is characterised by external bubble nucleation. These bubbles shatter near the edge of the jet leaving a significant liquid core of finite length immediately downstream of the exit orifice, beyond which complete disintegration of the jet creates a distinctive wide-angled spray.

Kitamura et al. [9] define critical superheat for flashing as the temperature at which the jet break-up mechanism presented by condition B occurs. This condition is characterised by an initial unbroken jet of finite length at which point it shatters suddenly and violently. The length of the unbroken jet corresponds to a period of delay during which bubble nuclei initially survive before growing rapidly causing the jet to disintegrate completely. This distance is not fixed, but is observed to fluctuate rapidly and randomly between approximately 0.5–3 nozzle diameters downstream.

This break-up regime was largely confined to releases from 1 and 2 mm nozzle diameters where it occurred in sequence after the inception of condition A. It is suggested that the size of the nozzle diameter in these cases in some way restricted bubble growth upstream of the exit orifice. Though it was observed to occur in releases from 3 and 4 mm nozzle diameters, it occurred very briefly and with a very short break-up length, if any at all. For this reason data points identifying this break-up mechanism were not included for these orifices.

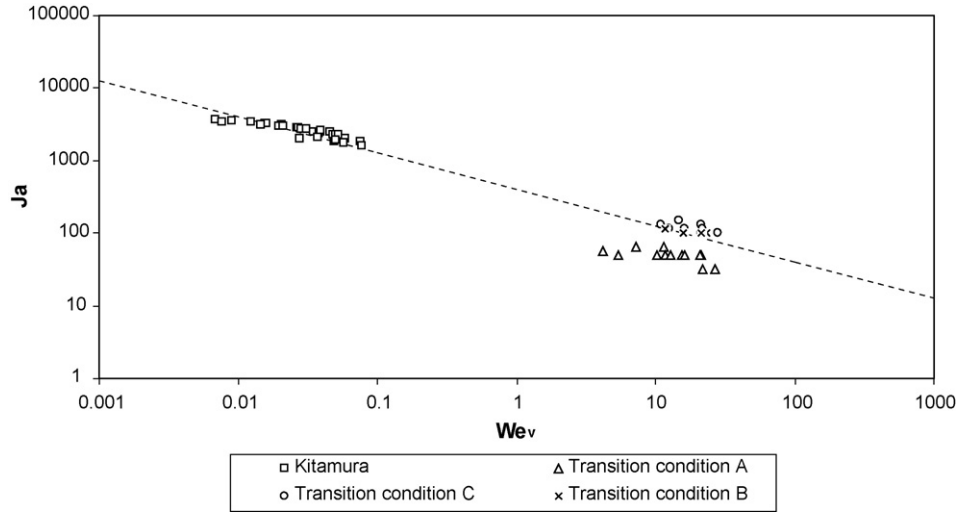

Fig. 10. Critical Jakob number for flashing as a function of vapour Weber number.

Condition C essentially represents the point beyond which the structure of the flashing jet does not significantly change, and is characterised by a barrel shaped spray, with violent jet disintegration at the nozzle with no delay time for bubble nucleation. This indicates upstream bubble nucleation, either by homogenous nucleation via molecular processes throughout the body of the fluid, or by heterogeneous nucleation at the liquid/nozzle wall interface. Conditions which govern transition between break-up phenomena can be predicted by a relatively simple relationship between Jakob and Weber number.

In Fig. 10 the degree of superheat has been non-dimensionalised by the Jakob number and the jet velocity has been non-dimensionalised using the vapour Weber number. From this figure it can be clearly seen that transition to condition B agrees reasonably well with the critical superheat for flashing as defined by Kitamura et al. [9]. This relationship is expressed in Eq. (10). However, in order to facilitate the application of this transition criterion to other liquids, it is necessary to develop this relationship further.

$$Ja = 400\, We_{\mathrm{v}}^{-0.5} \tag{10}$$

Kitamura et al. [9] modify the Jakob number by the liquid to vapour density ratio based on the need to introduce the effect of bubble growth rate on jet break-up, as this will depend on the liquid properties. This is achieved by the introduction of a correction factor, which compensates for the discrepancy between theoretical and measured bubble growth rates. This is presented in Fig. 11.

The far-left dataset in Fig. 11 is Kitamura's data for water. The middle dataset is Kitamura's data for ethanol. The far right dataset is Brown and York's dataset [8] for water and Freon-11, represented by un-shaded and shaded data points, respectively. One advantage of adopting the form of this correlation is that it is representative of transition to flashing for both water and ethanol. For this reason, this form of the correlation is adopted for modelling purposes. Fig. 12 presents this correlation in relation to the measured data and Kitamura's dataset.

Condition A is considered to be representative of the first transition stage where mechanical processes cease to dominate break-up. Kitamura's dataset for water closely correlates with the measured data for transition to condition B. This is considered as an intermediary stage of transition where full flashing characterised by upstream bubble growth has not yet began. This is represented by condition C. The correlations governing transition to conditions A and C are presented by Eqs. (11) and (12).

$$Ja\,\phi = 55\, We_{\mathrm{v}}^{-1/7} \tag{11}$$

$$Ja\,\phi = 150\, We_{\mathrm{v}}^{-1/7} \tag{12}$$

4. Model governing transition from mechanical break-up to full flashing

The data presented has been combined to produce a model that governs transition from mechanical break-up to full flashing of sprays, and example of which is presented in Fig. 13. In this case the release pressure is 10 bar and the orifice diameter is 1 mm (aspect ratio = 3.4 mm). Transition conditions A and C are represented by vertical dashed lines.

The model was developed by assuming a linear relationship between superheat and droplet SMD during the intermediary stage of transition. The final data point in the mechanical

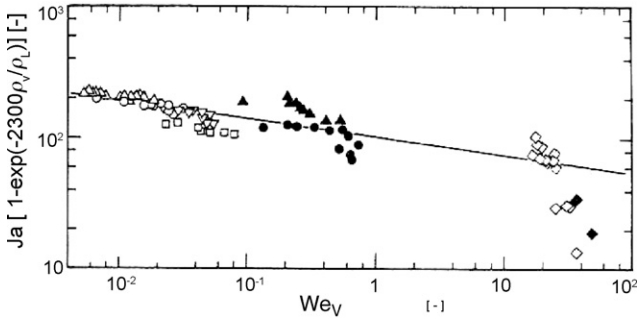

Fig. 11. Kitamura transition criteria [9].

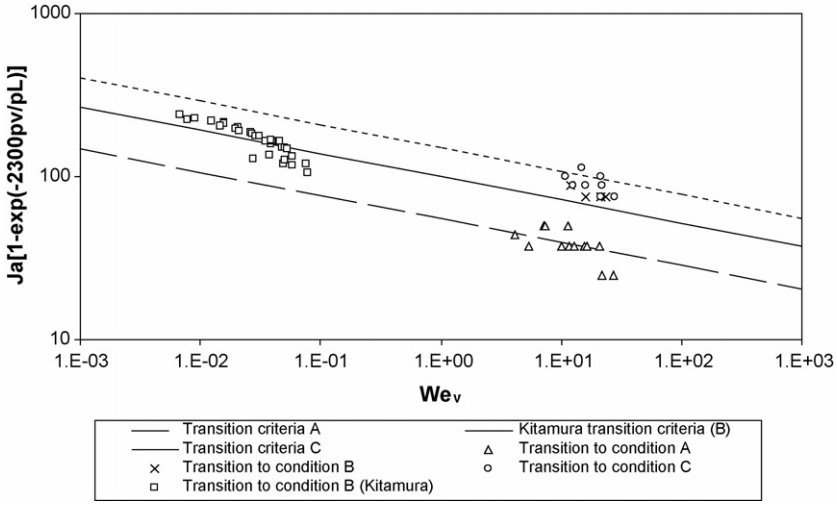

Fig. 12. Correlations for transition to the three identified stages of transition.

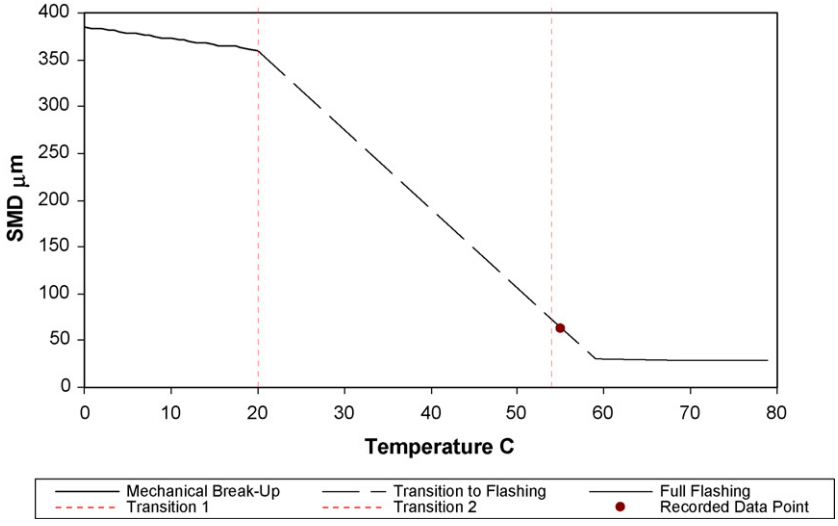

Fig. 13. Transition from mechanical break-up to full flashing (10 bar guage, nozzle = 1 mm).

break-up regime as determined by the proposed sub-cooled droplet correlation was taken as the beginning of this intermediary stage. A linear relationship was then superimposed to intercept the measured droplet SMDs for full flashing at 250 mm downstream of the exit orifice. It is difficult to obtain high quality atomisation with droplet SMDs of 30 μm or less, even with dynamic processes such as those which occur during superheated releases [17]. For this reason the linear relationship was extrapolated until a droplet SMD of 30 μm was reached, after which it was assumed that droplet size will decrease slowly at a nominal rate of 1 μm for every further 10 °C increase in superheat.

In order to extend the model to the full range of possible initial conditions it is recommended at this stage of development that the ratio of droplet SMD at the first to the final transition point (here taken to be 2.4), as demonstrated in Fig. 13, be adopted for all potential release scenarios.

The full model is presented mathematically in the accompanying paper [12].

5. Conclusions

- A new non-dimensionalised correlation for prediction of mean droplet size in isothermal water jets released in the mechanical break-up regime has been developed based on Phase Doppler Anemometry data.
- New correlations for the prediction of droplet size distribution in sub-cooled and fully flashing jets have also been developed using the data developed using this technique.
- A quantitative experimental methodology for identifying transition from mechanical break-up to full flashing has been designed and implemented, allowing comparison of transition data for cases more characteristic of atmospheric dispersion releases (higher Weber number) with a correlation previously presented in the literature by Kitamura.
- Using a similar transition criterion to that adopted by Kitamura, the current dataset is consistent with the correlation advocated by Kitamura based on Jakob number and Weber number.

- It is proposed that the modified correlation proposed by Kitamura, based on bubble-growth rates, is used until a broader dataset for a range of material releases becomes available.
- Three distinctive stages of transition have been identified for the break-up of superheated jets from the mechanical regime to full flashing. Two equations governing the starting point and end point of transition have been produced and recommended for modelling purposes.
- These results have been combined to produce an overall model for the full transition of a pressurised release of liquid from the mechanical break-up regime to full flashing.
- As the large majority of the data is for the case of water, the lack of data for different materials is considered the most significant deficiency at this stage of understanding. Hence, although an improvement on previous models for superheated releases, there is still considerable research and development required to appraise, consolidate and develop some of the assumptions and modelling approaches adopted in this paper. Furthermore, the concurrent measurement of source spray conditions with measured rainout has not been undertaken in this series.

References

[1] S.A. Ramsdale, Droplet formation and rainout from two phase flashing jets, AEA Technology, 1998.
[2] D.B. Harmon, Drop sizes from low speed jets, Franklin Inst. J. 259 (6) (1955) 519–522.
[3] H. Hiroyasu, T. Takoda, Fuel droplet size distribution in a diesel combustion chamber, SAE Trans., Paper 74017, 1974.
[4] A.C. Merrington, E.G. Richardson, The break-up of liquid jets, Proc. Phys. Soc. Lond. 59 (33) (1947) 1–13.
[5] Y. Tanasawa, S. Toyoda, On the Atomisation of a Liquid Jet Issuing From a Cylindrical Nozzle, No. 2, vol. 19, Tech. Report of Tohoku University, Japan, 1955, p. 135.
[6] J.N. Tilton, C.W. Farley, Predicting liquid jet break-up and aerosol formation during the accidental release of pressurised hydrogen fluoride, Plant/Operat. Progr. 9 (12) (1990) 120.
[7] M.M. Elkotb, Fuel atomisation for spray modelling, Progr. Energy Combust. Sci. 8 (1) (1982) 61–91.
[8] R. Brown, J.L. York, Sprays formed by flashing liquid jets, A.I.Ch.E. J. 8 (2) (1962) 149–153.
[9] Y. Kitamura, H. Morimitsu, T. Takahashi, Critical superheat for flashing of superheated liquid jets, Ind. Eng. Chem. Fundam. 25 (2) (1986) 207–211.
[10] R. Muralidhar, G.R. Jersey, F.J. Krambeck, A two-phase model for subcooled and superheated liquid jets, in: Proceedings of the International Conference and Workshop on Modelling and Mitigating the Accidental Releases of Hazardous Materials, AIChE, CCPS, New Orleans, LA, September 26–29, 1995, pp. 189–224.
[11] B.S. Park, S.Y. Lee, An experimental investigation of the flash atomisation mechanism, Atomis. Sprays 4 (1994) 159–179.
[12] H.W.M. Witlox, M. Harper, P.J. Bowen, V.M. Cleary, Flashing liquid jets and two-phase droplet dispersion. II. Comparison and validation of droplet size and rainout formulations, J. Hazard. Mater. (2006).
[13] T.R. Ohrn, D.W. Senser, A.H. Lefebvre, Geometrical effects on discharge coefficients for plain orifice atomisers, Atomis. Sprays 1 (2) (1991) 137–153.
[14] J.M. Buchlin, M. St. Georges, Detailed single spray experimental measurements and one dimensional modelling, Int. J. Multiphase Flow 20 (6) (1994) 979–992.
[15] A. Maragkos, Combustion hazard quantification of accidental releases of high-flashpoint liquid fuels, PhD Thesis, University of Wales, Cardiff, 2002.
[16] D.W. Johnson, J.L. Woodward, Release A Model with Data to Predict Aerosol Rainout in Accidental Releases, Center for Chemical Process Saftey (CCPS), New York, 1999.
[17] A.H. Lefebvre, Atomisation and Sprays, Hemisphere Publishing, 1989.